Proceedings of the TMCE 2006, April 18–22, 2006, Ljubljana, Slovenia, Edited by Horváth and Duhovnik

FAULT CLASSIFER DESIGN FOR HYDRAULIC CYLINDER DRIVE USING MATHEMATICAL FAULT MODELS

Ville Vidqvist
VTT Industrial Systems
VTT Technical Research Centre of Finland
Finland
ville.vidqvist@vtt.fi

ABSTRACT

Computer based modeling and simulation is becoming a regularly used tool for the design of hydraulic machinery. The same computer model can be used to design appropriate means for machine condition monitoring. The model can be also used to examine failure conditions. The acquired information is valuable for fault detection and diagnostics. Sometimes simulation can be the only feasible approach for fault threshold setting, since testing might be dangerous or expensive or machine has been updated and no previous fault measurements are available. In this paper simulation model was used to study efficiency of different classifiers in electrical signal failure, control valve sticking, as well as different leaking faults in position feedback valve-controlled hydraulic cylinder. 100 modified simulation runs were performed for each fault and different statistical windows were tested for feature extraction. The windowed data was used to test linear, quadratic, Parzen and neural network based classifiers.

KEYWORDS

hydraulics, fluid power, fault classifier, Bayes theory, neural network, Parzen window

1. INTRODUCTION

In the design phase of machines operating with hydraulics, virtual testing is coming more common. The system is modeled with computer and design parameters can be defined without the use of real world prototypes. Especially elasticity related dynamical properties can be accessed. Modeling can also be used to design condition monitoring methods for machinery. Modeling can also be used to failure simulation. Measurement information can be accessed cost-efficiently using virtual measurement instead of real sensors in real machines. This information can be used to design automatic fault diagnostic algorithms or fault classifiers (Leonhardt S. and Ayobi, M., 1997). Sometimes this might be the only way to design fault classifiers, since faults have a low probability of occurrence. It may take several years for critical faults to emerge. A common problem in process industry (e.g. energy production, paper production and steel production) is that machinery has been updated or modified, which makes the measured history data at least partially outdated. A common reason is also that measurement of faults is too dangerous or expensive. Main users of design tools are original equipment manufacturers (OEMs) They are widely moving to service business as the cash flow is more stable than in selling and margins are better. This lays groundwork for simulation based design of condition monitoring methods

Pattern recognition and hydraulic servo controls are widely researched fields. Applied mathematical methods are basically the same in both fields. The control theory tries to diminish step response oscillation while pattern recognition tries to find optimal method for extracting overlapping signal information. Not much has been done upon pattern recognition in fault diagnostics of hydraulics. Automotive industry is being active in analyzing electro-hydraulic steering and breaking components (Börner M. et al., 2002; Hahn, J-O. et al., 2002). Parameter variation has been examined in a case of simple hydraulic motor drive model (Yu, D., 1997). Models related to leaking have recently raised interest. The use of Kalman filtering in hydraulic leakage detection (An, L. and Sepehri, N., 2004) and QFT (Quantitative Feedback Theory) fault tolerant control under leakage (Karpenko, M. and Sepehri, N., 2004) has also been studied. The issues such as supply pressure and sensor faults as well as fluid contamination have been studied in relation to QFT-fault tolerant control (Niksefat, N. and Sepehri, N., 2002) and by using Volterra nonlinear models (Tan, H-Z. and Sepehri, N., 2002).

Measurement of pressure over filter is usually the only method for hydraulic system monitoring. Fluid condition is sometimes monitored. Usually laboratory analysis are used, since development of on-line oil quality measuring sensors is relatively slow and difficult (Parikka, R. et al., 2004; Parikka, R and Tervo, J., 2003). The major improvements have been made in the fields of moisture sensors and dielectric constant measuring sensors. Marine-, off-shore- and paper-industries have an increasing interest towards low cost humidity (or water content) in oil measurement devices. The viewpoint of the present paper is that the available on-line measurement methods are not yet cost-efficient to monitor hydraulic fluid powered machinery. More information is needed for early fault detection and reliable fault diagnostics. Viewpoint includes also the use of fewer sensors with increased intelligence. The increase of intelligence can be achieved mainly by modeling and simulation.

2. DESCRIPTION OF THE TARGET

The analyses were carried with feedback servo-proportional controlled cylinder drive model using semi-empirical parameters (Handroos, H., 1990). Model was developed from earlier work (Vidqvist V. and Tervo, J., 2005) by adding pressure relief valve and more advanced friction model. The model was created using Matlab R11 Simulink building blocks.

2.1. Model description

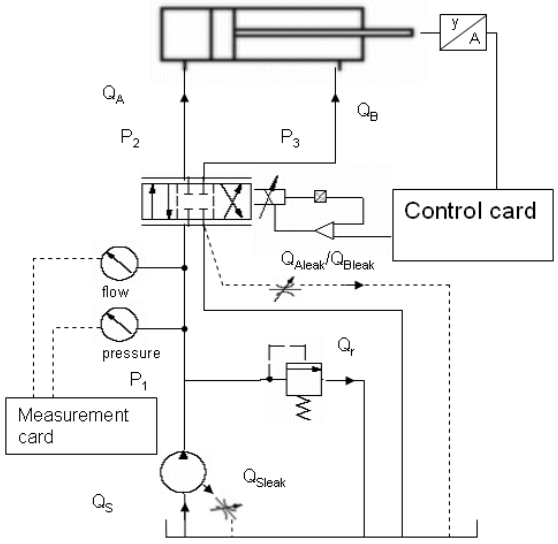

Figure 1 Main parameters of the model

The parameters in Figure 1 are as follows:

y = piston position [m]
p_1 = pressure prior to control valve [Pa]
p_2 = cylinder-side pressure [Pa]
p_3 = piston-side pressure [Pa]
Q_S = flow from pump [m^3/s]
Q_{Sleak} = leak flow from pump [m^3/s]
Q_r = flow from relief valve to tank [m^3/s]
Q_{Aleak}, Q_{Bleak} = leak flow from valve to tank [m^3/s]
Q_A = cylinder-side flow [m^3/s]
Q_B = piston-side flow [m^3/s]

Simulation model uses cylinder friction model that was generated originally for sliding pair contact (Canudas de Wit, C. et al., 1995; Canudas de Wit, C., 1998):

$$\begin{cases} F_\mu = \sigma_0 z + \sigma_1 \dot{z} + b\dot{y} \\ \sigma_0 = F_{St} / z_{\max} \\ \sigma_1 = \sqrt{m\sigma_0} \end{cases} \quad (1)$$

where,
F_μ = friction force [N]
σ_0 = spring coefficient of piston seal [N/m]
z = seal deflection [m]
$\dot{z}$ = speed of deflection change [m/s]
σ_1 = damping coefficient of piston seal [Ns/m]
b = coefficient of viscous friction [Ns/m]
$\dot{y}$ = piston velocity [m/s]

The supply force produced by cylinder:

$$F_{Su} = A_C p_2 - A_P p_3 - F_\mu \quad (2)$$

where,
F_{su} = supply force [N]
A_C= cylinder-side area of piston [m^2]
A_P= piston-side area of piston [m^2]

Cylinder is placed vertically towards ground, which leads to mechanism equation:

$$F_{Su} = mg \quad (3)$$

where,
m = combined mass of piston and load [kg]
g = gravitational coefficient [m/s^2]

Pressures are following:

$$\begin{cases} \dot{p}_1 = \dfrac{B_{e1}}{V_{10}}(Q_S - Q_r - Q_A - Q_B) \\ \dot{p}_2 = \dfrac{B_{e2}}{V_{20} + A_C y}(Q_A - Q_{Aleak} - A_C \dot{y}) \\ \dot{p}_3 = \dfrac{B_{e3}}{V_{30} + A_P (L - y)}(Q_B - Q_{Bleak} + A_P \dot{y}) \end{cases} \quad (4)$$

where

$\dot{p}_1, \dot{p}_2, \dot{p}_3$ = pressure differentials [Pa/s]

V_{10}, V_{20}, V_{30} = constant volumes related to different pressure [m^3]

B_{e1}, B_{e1}, B_{e1} = Effective bulk modulus values related to different pressure [Pa]

L = Stroke of piston [m]

The bulk modulus of casing prior to control valve is assumed to be infinitely high (rigid), which leads to following effective bulk modulus:

$$B_{e1} = B_o \,, \tag{5}$$

where

B_o = Bulk modulus of oil [Pa]

Pipes are used after control valve. For the calculation of cylinder and piston side effective bulk modulus values, piston is positioned to L/2. Bulk modulus values are as follows:

$$\begin{cases} \dfrac{1}{B_{e2}} = \dfrac{1}{B_o} + \dfrac{1}{B_p}\dfrac{V_{20}}{V_{t2}} \\ \dfrac{1}{B_{e3}} = \dfrac{1}{B_o} + \dfrac{1}{B_p}\dfrac{V_{30}}{V_{t3}} \end{cases}, \tag{6}$$

where

B_p = bulk modulus of pipe [Pa]

V_{t2}, V_{t3} = total volume for effective bulk modulus calculation (y =L/2) [m^3]

The dynamics of control valve is expressed as a second-order system between the spool displacement and the input voltage:

$$\begin{cases} \ddot{x} = U(t)\omega_v{}^2 - x\omega_v{}^2 - 2\dot{x}\delta_v\omega \\ \omega_v = \dfrac{1}{\tau_2} \\ \tau_1 = \dfrac{\tau_2}{\left|G\right|_{\omega-90°}} \\ \delta_v = \dfrac{\tau_1}{2\tau_2} \end{cases} \tag{7}$$

where

x = spool position [m]

$\dot{x}$ = spool velocity [m/s]

$\ddot{x}$ = spool acceleration [m/s^2]

U(t)= voltage input to valve [V]

ω_v = nominal angular velocity (frequency) in valve dynamics [rad/s]

δ_v = cancellation ratio of valve dynamics

$\left|G\right|_{\omega-45°(5\%)}, \tau_1, \tau_2$ = Valve coefficients

Cylinder side flow and leak flow are defined as follows:

$$\begin{cases} Q_A = C_v \cdot U \cdot sign(p_1 - p_2) \cdot \sqrt{\left|p_1 - p_2\right|} & U > 0 \\ Q_A = C_v \cdot U \cdot sign(p_2 - p_T) \cdot \sqrt{\left|p_2 - p_T\right|} & U \le 0 \\ Q_{Aleak} = \dfrac{v_{alle}}{2}\dfrac{Q_N}{P_{Ns}}(p_2 - p_t) & U > 0 \\ Q_{Aleak} = 0 & U \le 0 \end{cases} \tag{8}$$

where

C_v = valve semi-empiric flow coefficient [$m^3/(sV(Pa)^{0.5})$]

p_T = tank pressure [Pa]

v_{alle}= total leak flow relative to maximal flow [%]

Q_N=nominal flow through valve [m^3/s]

p_{Ns}=nominal input pressure of valve [Pa]

U=control voltage of valve [V]

Piston side flow is defined correspondingly as follows:

$$\begin{cases} Q_B = C_v \cdot U \cdot sign(p_T - p_3) \cdot \sqrt{\left|p_T - p_3\right|} & U > 0 \\ Q_B = C_v \cdot U \cdot sign(p_3 - p_1) \cdot \sqrt{\left|p_3 - p_1\right|} & U \le 0 \\ Q_{Aleak} = 0 & U > 0 \\ Q_{Aleak} = \dfrac{v_{alle}}{2}\dfrac{Q_N}{P_{Ns}}(p_3 - p_t) & U \le 0 \end{cases} \tag{9}$$

Flow from pump is as follows:

$$Q_S = \eta_S \cdot V_{Srev} \cdot n_S \tag{10}$$

where

η_S= volumetric efficiency of pump

V_{Srev}= pump displacement [m^3/rev]

n_s=pump speed [rev/s]

Flow through pressure relief valve follows normal valve flow equation and is:

$$Q_r = k_r \cdot sign(p_1 - p_T) \cdot \sqrt{\left|p_1 - p_T\right|} \tag{11}$$

where

k_r = amplification coefficient of relief valve

Dynamics of relief valve is expressed through relief valve amplification coefficient as a first order system as follows (Handroos, H., 1990):

$$\dot{k}_r = \frac{\left(p_1 - p_{ref}\right) - \left(C_1 + C_2 p_1\right) \cdot k_r}{C_{dyna}} \tag{12}$$

where
p_{ref} = reference pressure of relief valve [Pa]
C_1,C_2,C_{dyna} = semi-empirical coefficients of relief valve

Earlier work (Vidqvist V. and Tervo, J., 2005) included digital control properties, which were discarded. Also the look-up table based controller was replaced with PI-controller.

2.2. Fault Modeling

Following faults were included in the model:

- Electrical signal failure
- Valve spool sticking (jamming)
- Leak from cylinder side to outside system
- Leak from piston side to outside system
- Cylinder inside leak

Electrical signal was modeled by setting input voltage to zero for predefined time:

$$U(t) = 0, \quad t_{0Vstart} \le t \le t_{0Vend} \tag{13}$$

where
$t_{0Vstart}$ = start time of electrical signal failure [s]
t_{0Vend} = end time of electrical signal failure [s]

Valve spool sticking was modeled through voltage. The voltage value was kept constant for predefined time:

$$U(t) = U(t_{jamstart}), \quad t_{jamstart} \le t \le t_{jamend} \tag{14}$$

where
$t_{jamstart}$ = start time of spool sticking [s]
t_{jamend} = end time of spool sticking [s]

Cylinder side leak was modeled using a round hole as flow orifice to outside the system:

$$Q_{Aof} = Q_A - Q_{hole}(p_x = p_2, p_y = p_{air}) \tag{15}$$

where
Q_{Aof} = Valve flow under cylinder side leak [m^3/s]
Q_{hole} = Leak flow through hole [m^3/s]
p_{air} = atmospheric pressure [Pa]

Piston side leak was modeled correspondingly:

$$Q_{Bof} = Q_B - Q_{hole}(p_x = p_3, p_y = p_{air}) \tag{16}$$

where
Q_{Bof} = Valve flow under piston side leak [m^3/s]

A leak inside affects both flows as follows:

$$\begin{cases} Q_{Aif} = Q_A + Q_{hole}(p_x = p_2, p_y = p_3) \\ Q_{Bif} = Q_B - Q_{hole}(p_x = p_2, p_y = p_3) \end{cases} \tag{17}$$

where
Q_{Aif}, Q_{Bif} = Valve flow under inside leak [m^3/s]

The flow through the hole during leaking is calculated in the following way (both laminar and turbulent flows included) (Backé, W. 1986; Merrit, H. 1967; Rowe, W. 1984):

$$\begin{cases} Q_{hole}(p_x, p_y) = sign(p_x - p_y)\dfrac{-K_L\dfrac{128\nu\rho}{\pi} + \sqrt{\left(K_L\dfrac{128\nu\rho}{\pi}\right)^2 + 4\left(K_T\dfrac{8\rho}{\pi^2}(p_x - p_y)\right)}}{2K_T\dfrac{8\rho}{\pi^2}} \\ K_L = \dfrac{l_{hole}}{d_{hole}^4} \\ K_T = \dfrac{\zeta_{hole}}{d_{hole}^4} \end{cases} \tag{18}$$

where
ρ = density of oil [kg/m^3]
ν = kinematic viscosity of oil [m^2/s]
l_{hole} = length of the hole [m]
d_{hole} = diameter of the hole [m]
ξ_{hole} = flow resistance coefficient of the hole

3. METHODS

Signals generated with Simulink were analyzed using Matlab and its toolboxes. Pattern recognition toolbox (Prtools 3.16) was used to generate and test classifiers (Duin, R.P.W., 2000). Feature extraction was performed using statistical windows calculated data. Four classifiers were chosen to analyze data with different window sizes.

3.1. Generation of Simulated Signals

Simulink used variable step size for simulation runs. Duration of the Model was 3.5 s. Piston was driven to 0.4 m from 0 m position and back using ramp as control signal. Model signals were linearized to 20000 points. Noise signal was added to position feedback signal. Model used a random number generator with 0.15 s sample time. Noise signal was set to about +/- 1 mm. Gaussian distribution was used to generate the signal through random generator. 100 simulation runs were performed for each five fault in addition to 'no fault'-case. Faults were modified using random number generator with different feed. Fault variation is presented in Table 1.

Table 1 Table 1. Fault variation in simulation runs

	Model (0-3.5 s)
leaks	t_{start}: whole simulation [s] t_{stop}: whole simulation [s] d_{hole}: 5e-5+0...1*5e-4 [m]
sticking faults	t_{start}: round(0...1)*2+0.4+0...1*0.85 [s] t_{stop}: t_{start}+0.1+0...1*0.1 [s]
zero volt faults	t_{start}: round(0...1*3)+0.3+0..1*0.15 [s] $t_{stop:}$ t_{start}+0.1+0...1*0.1 [s]

3.2. Feature Extraction

Statistical windowing was chosen for feature extraction method. The statistical parameters used for windows are explained in Table 2.

Table 2 Table 3. Explanation of statistical parameters for windows.

Parameter	**Calculation**	**Explanation**
iqr	$median(x_{i75\%})$ - $median(x_{i25\%})$	Iqr computes the difference between the 75th and the 25th percentiles of the sample. The iqr is a robust estimate of the spread of the data, since changes in the upper and lower 25% of the data do not affect it.
kurtosis	$k = \frac{E(x-\mu)^4}{\sigma^4}$	Kurtosis is a measure of how outlier-prone a distribution is. The kurtosis of the normal distribution is 3. Distributions that are more outlier-prone than the normal distribution have kurtosis greater than 3; distributions that are less outlier-prone have kurtosis less than 3.
skewness	$k = \frac{E(x-\mu)^3}{\sigma^3}$	Skewness is a measure of the asymmetry of the data around the sample mean. If skewness is negative, the data are spread out more to the left of the mean than to the right. If skewness is positive, the data are spread out more to the right. The skewness of the normal distribution (or any perfectly symmetric distribution) is zero.
mean	$\bar{x}_j = \frac{1}{n}\sum_{i=1}^{n} x_{ij}$	Mean calculates the sample average.
RMS	$rms = \sqrt{\frac{\sum_i x_i^2}{n}}$	The RMS of a sample is a scalar that gives some measure of its magnitude
max	$\max(x_i)$	Returns the largest elements along of an array
slope	$k = \frac{f(x_i)-b}{x_i}$	Slope defines if the values of sample are increasing or decreasing

Feature vectors (feature vector = total amount of points in linearized simulation vector divided with window size) were calculated for cylinder side pressure (p_2) and valve control voltage (U). Feature vector sizes of 20, 15, 10 and 5 were calculated in chronological order for both selected signals (in 5 point feature vector the window size is 20000/5=4000 and the first feature e.g. RMS value represent linearized signal between 0 and 3.5/20000*4000=0.7 s, second 0.7-1.4 s and so on). Also 100, 75, 50, 25 were defined for the U signal. Feature extraction algorithm calculated not even windows by leaving the last points out (e.g. 1333*15=19995).

3.3. Classification

Bayesian classifiers were tested in classification of feature vectors **x** generated with statistical windows. The likelihood functions of classes' ω_i (here 6) with respect to **x** in the l-dimensional feature space (here 5...100) follow the general multivariate normal density (Theodoris, S. and Koutrombas, K., 1999)

$$p(\mathbf{x}|\omega_i) = \frac{1}{(2\pi)^{l/2}|\Sigma_i|^{1/2}} \exp\left(-\frac{1}{2}(\mathbf{x}-\boldsymbol{\mu}_i)^T \Sigma_i^{-1}(\mathbf{x}-\boldsymbol{\mu}_i)\right), \quad i = 1,...,M \tag{19}$$

where $\boldsymbol{\mu}_i = E[\mathbf{x}]$ is the mean value of the ω_i class and Σ_i the $l \times l$ covariance matrix defined as

$$\Sigma_i = E\left[(\mathbf{x}-\boldsymbol{\mu}_i)(\mathbf{x}-\boldsymbol{\mu}_i)^T\right] \tag{20}$$

$|\Sigma_i|$ denotes the determinant of Σ_i and E[•] is the mean (or average or expected) value of a random variable. Equation 19 is preferable to work with logarithmic functions due to its exponential form. This result

$$g_i(\mathbf{x}) = \ln\left(p(\mathbf{x}|\omega_i)P(\omega_i)\right) = \ln p(\mathbf{x}|\omega_i) + \ln P(\omega_i) \tag{21}$$

or

$$g_i(\mathbf{x}) = -\frac{1}{2}(\mathbf{x}-\boldsymbol{\mu}_i)^T \Sigma_i^{-1}(\mathbf{x}-\boldsymbol{\mu}_i) + \ln P(\omega_i) + c_i \tag{22}$$

where c_i is a constant equal to $-(1/2)\ln 2\pi - (1/2)\ln|\Sigma_i|$. Eq. 22 can be expanded to

$$g_i(\mathbf{x}) = -\frac{1}{2}\mathbf{x}^T\Sigma_i^{-1}\mathbf{x} + \frac{1}{2}\mathbf{x}^T\Sigma_i^{-1}\boldsymbol{\mu}_i - \frac{1}{2}\boldsymbol{\mu}_i^T\Sigma_i^{-1}\boldsymbol{\mu}_i + \frac{1}{2}\boldsymbol{\mu}_i^T\Sigma_i^{-1}\mathbf{x} + \ln P(\omega_i) + c_i \tag{23}$$

term $\mathbf{x}^T\Sigma_i^{-1}\mathbf{x}$ indicates that decision curves are quadratic (e.g., ellipsoids, parabolas, hyperbolas, pairs of lines). For *l*>2 the decision surfaces become hyperquadratic. This classification is referred here as *quadratic classifier (*qdc is the used Prtools function*)* If the covariance matrix is the same in all classes, that is, $\Sigma_i = \Sigma$, the quadratic term and c_i will be same in all discriminant functions. *g(**x**)* can be redefined to form

$$g_i(\mathbf{x}) = \boldsymbol{\mu}_i^T\Sigma^{-1}\mathbf{x} - \frac{1}{2}\boldsymbol{\mu}_i^T\Sigma\boldsymbol{\mu}_i + \ln P(\omega_i) \qquad (24)$$

Hence $g_i(\mathbf{x})$ is a linear function of x, the decision surfaces become hyperplanes. This type of classification is referred here as *linear classifier* (ldc in prtools).An example of linear and quadratic classification is presented in Figure 2.

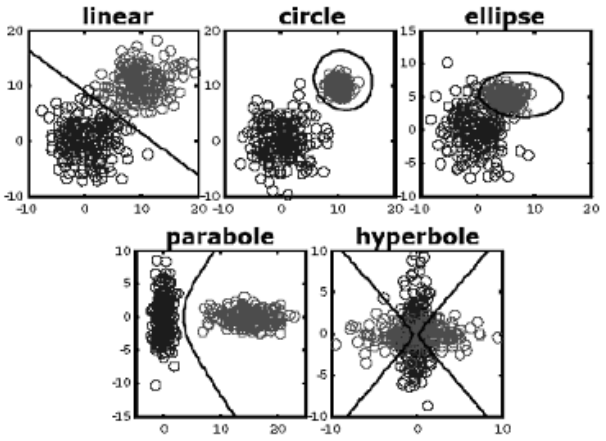

Figure 2 Linear and quadratic classification in the case of two class two feature space (Duin, R.P.W., 2000)

In addition to Bayesian based classifiers, *Parzen classifier* was tested for all feature vectors (parzenc). Density estimate is modified from Eq. 19 (Jain, A.K. and Ramaswami, M.D., 1988; Hamamoto, Y. et al., 1996)

$$p(\mathbf{x}|\omega_k) = \frac{1}{(2\pi)^{l/2}h_k|\Sigma_k|^{1/2}}\exp\left(-\frac{1}{2h_k^2}(\mathbf{x}-\boldsymbol{\mu}_k)^T\Sigma_k^{-1}(\mathbf{x}-\boldsymbol{\mu}_k)\right), \quad k=1,...,M$$

(24)

h_k is the parzen window size of class ω_k. Prtools use Lissack and Fu error estimate for the calculation of optimal window size (Lissack, T. and Fu, K.S, 1976).

Last classifier tested was *neural net classifier* (bpxnc in Prtools). Classifier is a feedforward two hidden layer network with batch mode updating using traditional sigmoid transfer function. Initialization is performed using Nguyen-Widrow method (Demuth, H. and Beale M., 1998; Nguyen, D. and Widrow, B., 1990). Calculations are based on backpropagation algorithm.

Forward computations are calculated after initialization for each training vector **x***(i), i*=1,2...,N (Theodoris, S and Koutrombas, K., 1999)

$$\upsilon_j^r(i) = \sum_{k=1}^{k_{r-1}}\omega_{jk}^r y_k^{r-1}(i) + \omega_{j0}^r \equiv \sum_{k=1}^{k_{r-1}}\omega_{jk}^r y_k^{r-1}(i) \quad r=1,2,...,L \;\; j=1,2,...,k_r$$

(25)

Cost function *J* is then updated

$$\begin{cases} J = \sum_{i=1}^{N}\varepsilon(i) \\ \varepsilon(i) \equiv \frac{1}{2}\sum_{m=1}^{k_L}e_m^2(i) \equiv \frac{1}{2}\sum_{m=1}^{k_L}\left(f(\upsilon_m^L(i) - y_m(i)\right)^2 \end{cases} \qquad (26)$$

after this backward computations are calculated

$$\delta_j^L(i) = e_j(i)f'(\upsilon_m^L(i) - y_m(i)) \quad i=1,2,...,N \;\; j=1,2,...,k_L$$

(27)

and in the sequel

$$\begin{cases} \delta_j^{r-1}(i) = e_j^{r-1}(i)f'(\upsilon_j^{r-1}(i) \quad r=L,L-1,...,2 \;\; j=1,2,...,k_r \\ e_j^{r-1}(i) = \sum_{k=1}^{k_r}\delta_k^r(i)\omega_{kj}^r \end{cases}$$

(28)

finally weights are updated

$$\begin{cases} \mathbf{w}_j^r(new) = \mathbf{w}_j^r(old) + \Delta\mathbf{w}_j^r \;\; r=1,2,...,L \quad j=1,2,...,k_r \\ \Delta\mathbf{w}_j^r = -\mu\sum_{i=1}^{N}\delta_j^r(i)\mathbf{y}^{r-1}(i) \end{cases}$$

(29)

where $\mathbf{w}_j^r = \left[\omega_{j0}^r, \omega_{j1}^r, ..., \omega_{jk_{r-1}}^r\right]$. Training is stopped by Prtools when iteration epochs are twice that of the best classification result. Number of output neurons equals the number of classes. Figure 3 illustrates the calculation procedure.

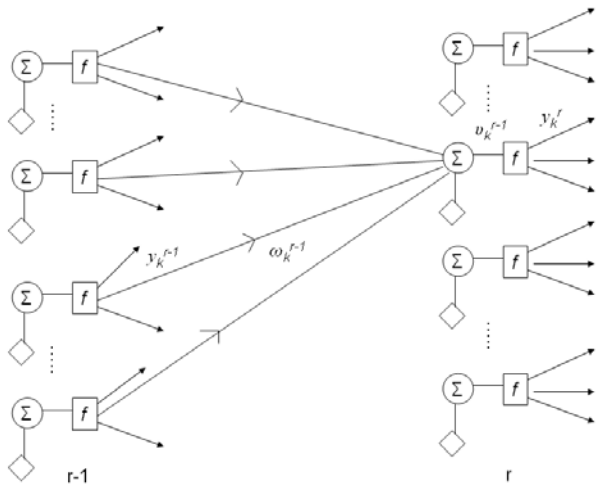

Figure 3 Definition of variables involved in the backpropagation algorithm

4. RESTRICTIONS OF STUDY

The assumptions made in this work are as follows (Handroos, H., 1990):

- The viscosity of oil, the bulk modulus of oil, the discharge coefficients and flow angles of valve orifices are constants
- Pressure is distributed evenly
- Pressure does not saturate or cavitate
- The inlet pressure of each valve is greater than or equal to outlet pressure and the tank pressure is zero
- the compressibility of oil in the damping chambers as well as the Coulomb and the viscous friction force between the valve spool or poppet and the valve housing can be neglected

The simulated parameters have not been verified by measurements. Although the values of the parameters do lack realism, it is expected that the estimated values are "close enough". (Virvalo, T., 1997; Virvalo, T., 1999; Handroos, H., 1990) As the classifiers function correctly with relatively noised data, the exact values are not necessarily needed. Similar hydraulic system models without faults have been verified previously (Virvalo, T., 1997; Virvalo, T., 1999; Handroos, H., 1990). Bulk modulus values of the model are not compensated by piston movement. The modulus values are calculated when the piston is in the middle position of the stroke. This is due to technical problems in calculation. Also the pressure relief valve model was reduced to first order model.

5. RESULTS

From 100 simulations (5+1 cases in each simulation) 80 random simulation runs were used for training (6*80=480) and the rest 20 simulations were used for classifier testing. Total amount of classifiers is 336 (voltage measurement quantity * 8 different feature vector sizes * 4 different classifiers * 7 different parameters for feature vectors + pressure quantity * 4 different feature vector sizes * 4 different classifiers * 7 different parameters for feature vectors). Results are presented in Appendices. Tables 3, 4 and 5 shows the fraction of incorrectly classified test for each method applied (higher than 0.5 value means that classifier performs worse than if the decision is made by tossing a coin).

6. DISCUSSION

A large amount of oil leaking out of the system is usually easily visible as fluid puddles under the machinery. This is especially the case when the hose is leaking. The situation is different in the case of pipe breakage or seal damage. The leak may be small enough to remain unnoticed. The oil consumption increases slightly, but not necessarily enough to arise any concerns. Even if the correct conclusions are made, finding the leak may be a tedious task.

Canudas De Wit model was used to model friction (eq. 1). A common model invented by Karnopp was used in work by Tan and Sepehri (2004):

$$F_\mu(\dot{y}) = F_C + (F_S - F_C)\cdot e^{-\left(\frac{\dot{y}}{v_S}\right)^2}\cdot \mathrm{sgn}(\dot{y}) + d\dot{y} \quad (30)$$

where
F_C = Coulomb friction [N]
F_S = static friction [N]
d = effective damping ratio [Ns/m]
v_S = the threshold for break away velocity for switching between static friction and slip friction [m/s^2]

$$\mathrm{sgn}(\dot{x}) = \dot{x}/|\dot{x}|, |\dot{x}| \neq 0; \mathrm{sgn}(\dot{x}) \in [-1,1], \dot{x} = 0$$

There are several reasons for using of the Karnopp model. It is quite simple, easy to understand and it is numerically efficient. Disadvantages include that actuator is drifting when outside load and friction load are in balance. In reality as well as in Canudas De Wit model, position is not affected. Complexity and definition of the parameter σ_1 are the disadvantages of the Canudas De Witt model.

Position (Fig. 4), valve control voltage (Fig. 5) and cylinder side pressure (Fig. 6) example for different faults are presented in Appendices. The pressure signals become negative in the case of inside leak. This is due to the limitations of the model, which does not compensate the rapid pressure fluctuations fast enough. Also the pressure relief valve flow was set so that negative flow is not possible (i.e. flow from tank to system). The sudden pressure increase in cylinder side leak fault at 1.5 s is due to elimination of negative flow.

The model was used to simulate faults in places where substantial effect can be seen. There is only a negligible visible effect on pressure if sticking takes place while the spool is not moving. Also in the case of zero volt-fault, the effect is minimal if the control voltage (flow) is already zero (see Table 1).

The zero-volt fault changes spool position very rapidly. This can be seen directly from the pressure change. Piston position is also heavily affected and the work cycle is delayed. Fluid leak to air (atmospheric pressure) produces some visible changes to the position signal. Reason for short time excessive over steering at 2 s is the negative flow aspect of the pressure relief valve mentioned before. Position is slightly over steered during cylinder side leak and under steered during piston side leak. Pressure increases as the closed loop system seeks balance between pressure and flow at near piston stroke position by adjusting the valve opening. Larger holes should produce pressure drop. Oscillation amplitudes are smaller during outside leaking near piston stroke position than in no fault case. Leaking inside the cylinder produces serious pressure oscillation. Pressure oscillation was so extensive that it induced oscillation to position signal. The kind of a variation in hydraulic system pressure is undesirable since it produces wear. Spool sticking produces moderate pressure oscillation after spool is released.

General requirement to keep measurement cost low was the reason for quantity selection for windows and classifiers. Flow sensors are expensive and flow information can be accessed more easily by measuring control voltage. Pressure measurement is moderately expensive, but it is less costly than flow measurement. As sensors are not needed in voltage measurement, it is the most preferable choice for monitoring purposes. Sensor price may be irrelevant as signal processing unit represent the highest cost of system.

Usually 20 % is defined as a minimum acceptable error probability of classifier (50 % is the probability for coin tossing). Using this definition the classification error probability of Tables 3, 4, 5 in almost all cases are acceptable. . Even zero error can be seen using voltage, 2000 point window (10 point feature vector) and maximum value of feature vector. Small windows (or large feature vector) were not tested for pressure signals. Feature matrices were singular, which stopped the classifier teaching algorithm. This is a common problem for classifiers (Hamamoto, Y. et al, 1996). Comparison of voltage and pressure signals does not show much difference in classification. Best window sizes seem to be 2000 points (10 point feature vector) or 1333 points (15 point feature vector) wide. Best results can be achieved using parameters like root mean square (RMS) or maximum value of the feature vector (max). These parameters are the most used also for elements of rotating machines in vibration condition monitoring (e.g. rolling bearings, gears). The Parzen classifier produced the smallest error in classifying voltage and cylinder side pressure data. Quadratic classifier was the best in classifying the data of piston side pressure signal. The results usually depend more on the feature extraction method than on the classifier type. In this work the linear and neural net classifiers performed worse than quadratic or Parzen classifiers. Faster linear classification might be wanted, despite worse performance. The neural network had two hidden layers. The amount of training vectors was 80. The network can have 75 or 100 input neurons (size of feature vector). Amount of training vectors should be ten times more with these sizes of networks. The idea was to test classifier with small amount of training vectors. Also the neural networks have drawbacks in convergence and local optimum (An, L. and Sepehri, N., 2004).

Some feature vectors are plotted in Appendices (Fig 7-13). X-value represent the feature vector (1,2,3,4...) and y-value represent the calculated feature value (e.g. RMS) of signal window in that feature vector value. Feature vector is plotted as constructed in chronological order of its signal. All constructed 100 vectors are plotted overlapping each other. This highlights the differences generated with fault variation (Table 1) and noise. Figures 7 and 8 visualize the effect of window size reduction to signal. RMS-feature vectors are plotted for sticking fault. Work cycle of valve voltage is not recognizable in 5 point vector, since too much signal information is lost (the original sticking fault voltage signal is

plotted in Fig. 5, RMS can not be negative). The effect is visible also in classifier results as 5 point vector performs worse (higher classification error value) than 10 or 15 point vectors (Tables 4, 5 last three columns). Excessive information like 100 or 75 point vectors also reduces classifier efficiency (Table 3 first two columns).

Figures 9 and 10 visualize the effect of windows parameter change to signal. The high sensitivity of kurtosis (as well as skewness) can be noticed as large variation in same feature point between feature vectors (Fig 10). Mean value is more stable (Fig. 9) Sensitivity of parameter decreases classifier efficiency (Hyötyniemi, H., 2001). In general, average efficiency of kurtosis and skewness (Tables 3, 4, 5, respective row) was worse than that of robust parameters like mean or RMS. The efficiency differences were over ten percentages.

Figures 11, 12 and 13 visualize effects of different faults to 20 points max feature vector. The clear visible difference between feature vector shapes in different figures show why the max parameter performed best in classification.

7. CONCLUSIONS

It has been demonstrated that statistical windows based data classification can be used for analyzing a hydraulic cylinder drive, which is essentially a nonlinear system. The modeled fault phenomena were not verified experimentally. Tested classification methods worked well on simulated faults like electrical signal failure, control valve sticking and leaking in feedback valve-controlled hydraulic cylinder. The used hydraulic component models have been verified in various previous research (Virvalo, T., 1997; Virvalo, T., 1999; Handroos, H., 1990). The smallest classification error was reached with the Parzen classifier. The analyzed parameter was the maximum value of control valve voltage signal, with window size of 2000 points (from 20000 points). In general root mean square (RMS) and maximum value of window (max) parameters functioned best with window sizes of 1333 points (15 points size feature vector) and 2000 points (10 points size feature vector). Parzen and quadratic classifiers performed better than linear and neural network based classifiers. There was not any significant difference in results, if the used quantity was control valve voltage or pressure.

APPENDICES

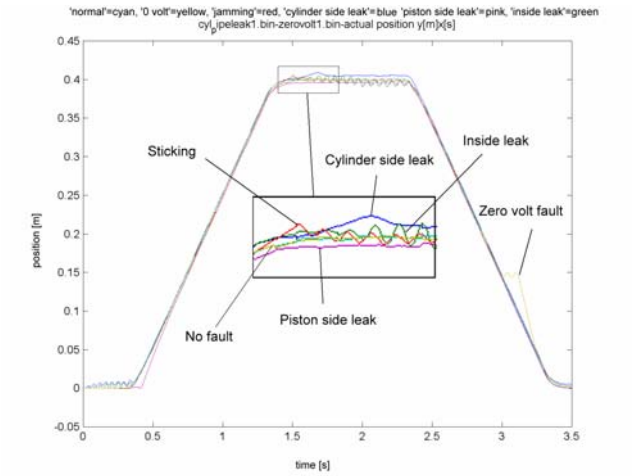

Figure 4 Position signal (y) example with different faults

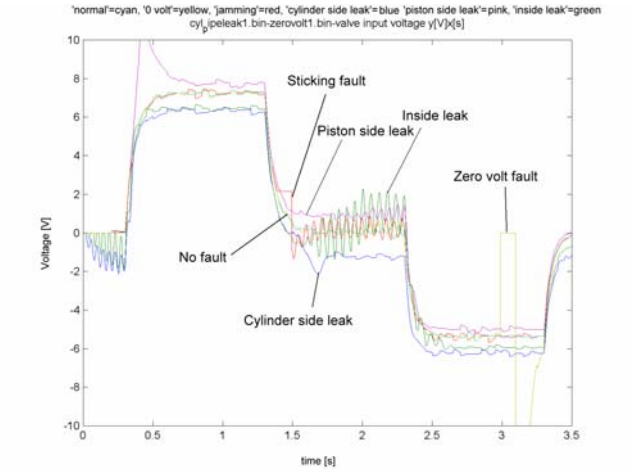

Figure 5 Valve control voltage (U) example with different faults

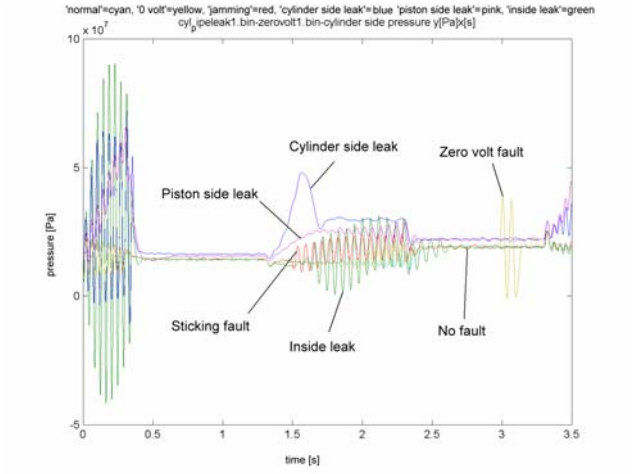

Figure 6 Cylinder side pressure (p_2) example with different faults

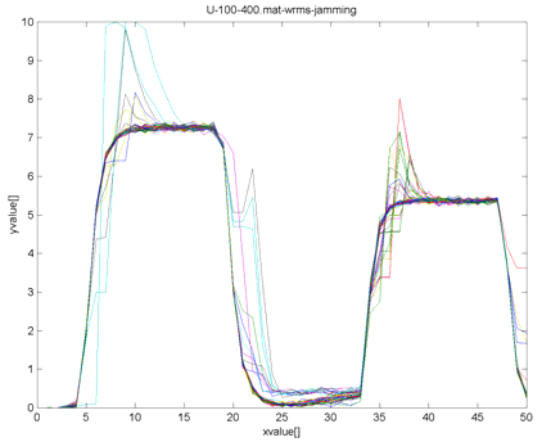

Figure 7 50 point (xvalue) valve control voltage (U) RMS (yvalue) feature vectors (100 plotted) for sticking fault-case

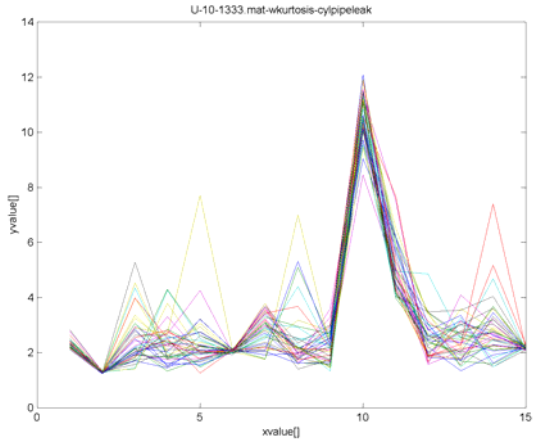

Figure 10 15 point (xvalue) valve control voltage (U) kurtosis (yvalue) feature vectors (100 plotted) for cylinder side leak case

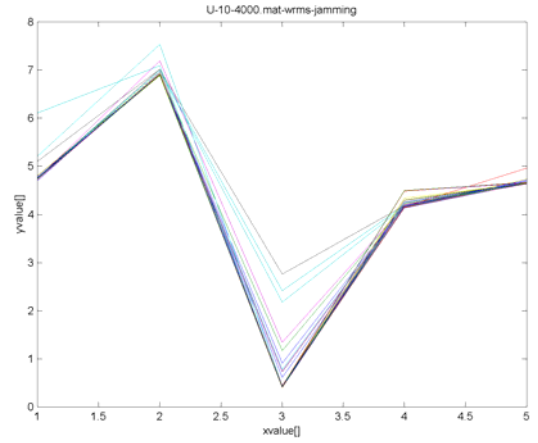

Figure 8 5 point (xvalue) valve control voltage (U) RMS (yvalue) feature vectors (100 plotted) for sticking fault-case

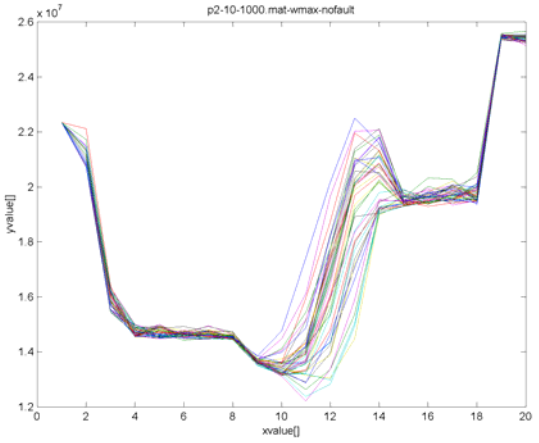

Figure 11 20 point (xvalue) cylinder side pressure (p_2) max (yvalue) feature vectors (100 plotted) for no fault-case

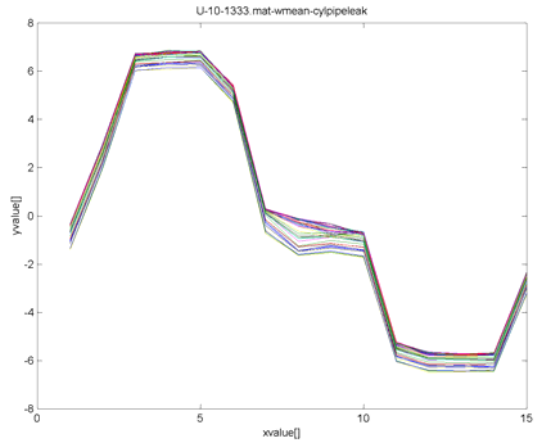

Figure 9 15 point (xvalue) valve control voltage (U) mean (y-value) feature vectors (100 plotted) for cylinder side leak case

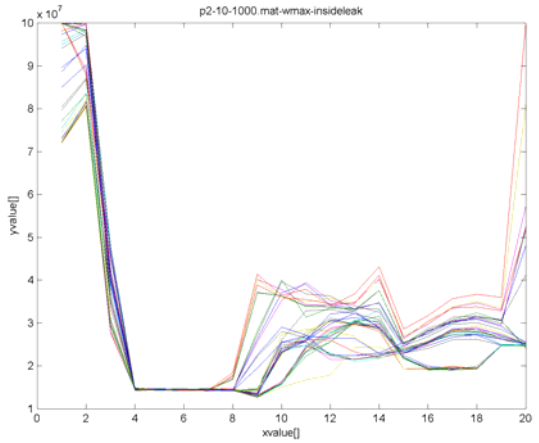

Figure 12 20 point (xvalue) cylinder side pressure (p_2) max (yvalue) feature vectors (100 plotted) for inside leak-case

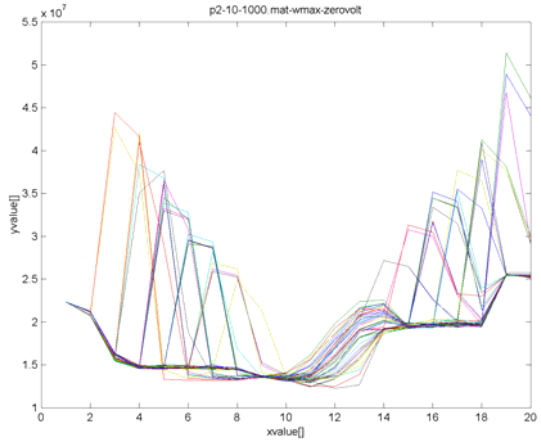

Figure 13 20 point (xvalue) cylinder side pressure (p_2) max (yvalue) feature vectors (100 plotted) for zero volt fault-case

Table 3 Control voltage (U) classifier error probability with 25-100 feature vector size (less is better)

Error probability, 5+1 faults, 100 vectors per fault, 480 learn and 120 test vectors

wsize from 20000 points	100 points	75 points	50 points	25 points
linear	U-10-200.mat	U-10-266.mat	U-10-400.mat	U-10-800.mat
iqr	0.1083	0.175	0.1167	0.325
kurtosis	0.0917	0.2	0.3333	0.3417
max	0.05	0.0833	0.125	0.1333
mean	0.1917	0.1	0.1083	0.2083
rms	0.15	0.1333	0.175	0.1333
skewness	0.1333	0.225	0.1917	0.1583
slope	0.15	0.1917	0.1583	0.2667
quadratic	U-10-200.mat	U-10-266.mat	U-10-400.mat	U-10-800.mat
iqr	0.2083	0.0583	0.0417	0.15
kurtosis	0.1167	0.1833	0.0917	0.2083
max	0.0333	0.0667	0.0833	0.2667
mean	0.0917	0.0417	0.05	0.1167
rms	0.05	0.0917	0.0333	0.175
skewness	0.0667	0.0917	0.1583	0.075
slope	0.05	0.0583	0.05	0.1417
parzen	U-10-200.mat	U-10-266.mat	U-10-400.mat	U-10-800.mat
iqr	0.0583	0.0417	0.05	0.1167
kurtosis	0.0917	0.0917	0.1833	0.0833
max	0.0333	0.0417	0.0333	0.0583
mean	0.1583	0.0917	0.075	0.05
rms	0.0833	0.075	0.0667	0.1083
skewness	0.0667	0.075	0.075	0.0583
slope	0.0833	0.0583	0.075	0.125
NN2hidden	U-10-200.mat	U-10-266.mat	U-10-400.mat	U-10-800.mat
iqr	0.0333	0.0583	0.1833	0.3833
kurtosis	0.2333	0.175	0.2917	0.3
max	0.0583	0.0583	0.0917	0.225
mean	0.3	0.175	0.15	0.25
rms	0.075	0.15	0.1167	0.1417
skewness	0.2833	0.1917	0.1667	0.3333
slope	0.1417	0.1167	0.1167	0.2417

Table 4 Control voltage (U) classifier error probability with 5-20 feature vector (less is better)

Error probability, 5+1 faults, 100 vectors per fault, 480 learn and 120 test vectors

wsize from 20000 points	20 points	15 points	10 points	5 points
linear	U-10-1000.mat	U-10-1333.mat	U-10-2000.mat	U-10-4000.mat
iqr	0.1417	0.1417	0.1333	0.2417
kurtosis	0.1583	0.1833	0.3167	0.35
max	0.0583	0.0917	0.0667	0.125
mean	0.1	0.1167	0.0667	0.2
rms	0.1667	0.125	0.0833	0.1167
skewness	0.175	0.225	0.1667	0.125
slope	0.2083	0.1583	0.1667	0.2667
quadratic	U-10-1000.mat	U-10-1333.mat	U-10-2000.mat	U-10-4000.mat
iqr	0.225	0.0417	0.0667	0.0833
kurtosis	0.2	0.15	0.0833	0.225
max	0.05	0.025	0.4083	0.2833
mean	0.075	0.0583	0.0417	0.1083
rms	0.05	0.025	0.05	0.1083
skewness	0.0917	0.125	0.1167	0.1167
slope	0.0417	0.025	0.0833	0.1333
parzen	U-10-1000.mat	U-10-1333.mat	U-10-2000.mat	U-10-4000.mat
iqr	0.1083	0.0833	0.075	0.0417
kurtosis	0.15	0.1333	0.1583	0.1
max	0.025	0.0167	0	0.0417
mean	0.0583	0.0833	0.05	0.1083
rms	0.0667	0.0667	0.0667	0.0833
skewness	0.0833	0.1167	0.0833	0.0417
slope	0.1	0.075	0.0583	0.15
NN2hidden	U-10-1000.mat	U-10-1333.mat	U-10-2000.mat	U-10-4000.mat
iqr	0.1583	0.125	0.1833	0.3667
kurtosis	0.2333	0.2167	0.25	0.3333
max	0.05	0.0917	0.0833	0.1
mean	0.125	0.2833	0.075	0.1917
rms	0.1667	0.275	0.175	0.15
skewness	0.15	0.2	0.2833	0.3
slope	0.1583	0.1833	0.1917	0.3083

Table 5 Cylinder side pressure (p_2) classifier error probability with 5-20 feature vector size (less is better)

Error probability, 5+1 faults, 100 vectors per fault, 480 learn and 120 test vectors

wsize from 20000 points	20 points	15 points	10 points	5 points
linear	p2-10-1000.mat	p2-10-1333.mat	p2-10-2000.mat	p2-10-4000.mat
iqr	0.0833	0.1167	0.0833	0.2333
kurtosis	0.1333	0.2667	0.25	0.4
max	0.05	0.0583	0.0833	0.1333
mean	0.125	0.1833	0.1333	0.1667
rms	0.075	0.15	0.0583	0.15
skewness	0.1417	0.1583	0.1917	0.1583
slope	0.1917	0.175	0.1333	0.2417
quadratic	p2-10-1000.mat	p2-10-1333.mat	p2-10-2000.mat	p2-10-4000.mat
iqr	0.1167	0.0583	0.0583	0.175
kurtosis	0.1333	0.1333	0.0917	0.175
max	0.0167	0.05	0.4083	0.275
mean	0.0583	0.0667	0.0417	0.1
rms	0.05	0.0333	0.025	0.15
skewness	0.0833	0.1	0.0833	0.0667
slope	0.0583	0.0833	0.05	0.1167
parzen	p2-10-1000.mat	p2-10-1333.mat	p2-10-2000.mat	p2-10-4000.mat
iqr	0.0583	0.0583	0.05	0.1083
kurtosis	0.1333	0.0833	0.1333	0.05
max	0.0583	0.0333	0.025	0.0333
mean	0.0833	0.1083	0.0667	0.0667
rms	0.0583	0.075	0.0417	0.1417
skewness	0.1	0.1	0.0917	0.0583
slope	0.0667	0.1167	0.0583	0.1083
NN2hidden	p2-10-1000.mat	p2-10-1333.mat	p2-10-2000.mat	p2-10-4000.mat
iqr	0.0917	0.0667	0.1583	0.2583
kurtosis	0.2	0.15	0.2917	0.3
max	0.25	0.05	0.1583	0.3917
mean	0.125	0.3	0.175	0.2083
rms	0.0417	0.1083	0.2583	0.1667
skewness	0.2417	0.1917	0.125	0.2917
slope	0.125	0.2917	0.1833	0.1583

REFERENCES

An, L., Sepehri, N., (2004), Leakage fault identification in a hydraulic positioning system using extended Kalman filter", American Control Conference, Proceedings of the Volume 4, 30 June, pp. 3088 - 3093

Backé, W., (1994), Grundlagen der Ölhydraulik, Vorlesungsscript, 10. edition, RWTH Aachen

Börner M., Straky, H., Weispfenning, T., Isermann, R., (2002), "Model based fault detection of vehicle suspension and hydraulic brake systems", Mechatronics, Volume 12, Issue 8, pp. 999-1010

Canudas de Wit, C., Olsson, H., Åström, K.J., Lischinsky. P., (1995), "a New Model for Control of Systems with Friction", IEEE Transactions on Automatic Control, Vol. 40, No. 3, pp. 419-425

Canudas-de-Wit, C., (1998), "Comments on a new model for control of systems with friction", Automatic Control, IEEE Transactions on volume 43, Issue 8, pp. 1189 - 1190

Demuth, H., Beale, M., (1998), Neural Network Toolbox for use with Matlab User's Guide Version 3.0, Mathsoft Inc., 742 pp.

Duin, R.P.W., (2000), PRTools_3, a Matlab Toolbox for Pattern Recognition, Delft University of Technology, January 2000

Hahn, J-O., Hur, J-W., Cho, Y.M., Lee K.I., (2002), "Robust observer-based monitoring of a hydraulic actuator in a vehicle power transmission control system", Control Engineering Practice, Volume 10, Issue 3, pp. 327-335

Hamamoto, Y., Fujimoto, Y, Tomita, S., (1996), "On the estimation of a covariance matrix in designing Parzen classifiers", Pattern Recognition 29(10): 1751-1759

Handroos, H. (1990), Methods for combining a theoretical and an empirical approach in modeling pressure and flow control valves for CAE-programs for fluid power circuits, Helsinki, Finnish Academy of Technology, 53 p.

Hyötyniemi, H., (2001), Multivariate regression - Techniques and tools. Helsinki, Finland: Helsinki University of Technology, Control Engineering Laboratory, 207 p.

Jain A. K., Ramaswami, M., D. (1988), "Classifier design with Parzen windows", Pattern Recognition and Artificial Intelligence, Elsevier, Amsterdam, pp. 211-228

Karpenko, M., Sepehri, N., (2005), "Fault-tolerant control of a servohydraulic positioning system with crossport leakage", Control Systems Technology, IEEE Transactions on Volume 13, Issue 1, pp. 155 - 161

Lissack, T., Fu, K.S., (1976), "Error estimation in pattern recognition via L^{α} − distance between posterior density functions. IEEE Transitions on Information Theory pp. 34–45

Leonhardt, S. Ayoubi, M., (1997), "Methods of fault Diagnosis", Control Engineering Practice, v 5, n 5, pp. 683-692

Merrit, H., (1967), Hydraulic Control Systems, USA, John Wiley and Sons Inc., 354 p.

Niksefat, N., Sepehri, N., (2002), "A QFT fault-tolerant control for electrohydraulic positioning systems", IEEE Transactions on Control Systems Technology, Volume 10, Issue 4, pp. 626 - 632

Nguyen, D., B. Widrow, (1990), "Improving the learning speed of 2-layer neural networks by choosing initial values of the adaptive weights," Proceedings of the International Joint Conference on Neural Networks, vol 3, pp. 21-26

Parikka, R., Vidqvist V., Vaajoensuu, E., (2004), "Low-cost analysers based on light transmittance for oil condition monitoring", AIMETA International Tribology Conference, 14-17 Sept, Rome, AITC, pp. 725 - 734

Parikka, R., Tervo, J., (2003), "Condition monitoring of oil in mobile machinery", Condition monitoring conference, Oxford, 2 - 4 July, Coxmoor Publishing. Oxford, pp. 400 - 407

Rowe, W.B., (1983), Hydrostatic and hybrid bearing design, Butterworth, London, 240 p.

Tan, H-Z., Sepehri, N., (2002), "Parametric fault diagnosis for electrohydraulic cylinder drive units", IEEE Transactions on Industrial Electronics Volume 49, Issue 1, pp. 96 - 106

Theodoridis, S., Koutroumbas, K., (1999), Pattern recognition Academic Press, San Diego, 625 p.

Virvalo, T., (1997), "Nonlinear model of analog valve", In the 5th Scandinavian International Conference on Fluid Power, Linköping, pp 199-214.

Virvalo, T., (1999), "On the Damping of a Hydraulic Cylinder Drive", Sixth Scandinavian International Conference on Fluid Power, SICFP'99, Tampere

Vidqvist, V., Tervo, J., (2005), "Computer Based Fault Modeling in Hydraulic Cylinder Drive", Condition monitoring and diagnostic engineering management conference, Bedfordshire, 30 August - 1 September, COMADEM, pp. 285-295

Yu, D., (1997), "Fault diagnosis for a hydraulic drive system using a parameter-estimation method", control Engineering Practice, Volume 5, Issue 9, pp. 1283-1291